PHYSICAL REVIEW B **89**, 121404(R) (2014)

Temperature- and density-dependent transport regimes in a *h*-BN/bilayer graphene/*h*-BN heterostructure

C. Cobaleda,[1] S. Pezzini,[1,2,*] E. Diez,[1] and V. Bellani[2]
[1]*Laboratorio de Bajas Temperaturas, Universidad de Salamanca, E-37008 Salamanca, Spain*
[2]*Dipartimento di Fisica and CNISM, Università degli studi di Pavia, I-27100 Pavia, Italy*
(Received 12 November 2013; revised manuscript received 21 January 2014; published 10 March 2014)

We report on multiterminal electrical transport measurements performed on a bilayer graphene sheet enclosed by two hexagonal boron nitride flakes. We characterize the temperature dependence of electrical resistivity from 300 mK to 50 K, varying the carrier densities with a back gate. The resistivity curves clearly show a temperature-independent crossing point at density $n = n_c \approx 2.5 \times 10^{11}$ cm^{-2} for both positive and negative carriers, separating two distinct regions with $d\rho/dT < 0$ and $d\rho/dT > 0$, respectively. Our analysis rules out the possibility of a zero-T quantum phase transition, revealing instead the onset of robust ballistic transport for $n > n_c$, while the T dependence close to the neutrality point is the one expected from the parabolic energy-momentum relation. At low temperature ($T \ll 10$ K), the data are compatible with transport via variable range hopping mediated by localized impurity sites, with a characteristic exponent $1/3$ that is renormalized to $1/2$ by Coulomb interaction in the high-density regime.

DOI: 10.1103/PhysRevB.89.121404 PACS number(s): 72.80.Vp, 71.30.+h, 73.23.Ad

AB-stacked bilayer graphene is a zero-gap semimetal with particle-hole symmetric parabolic bands. This system has attracted a great deal of attention since the early days of graphene science [1,2], especially owing to the prediction that a band gap can be open in a controllable way by breaking the layers' symmetry (i.e., making atomic sites on the upper and lower layers inequivalent), for instance by applying a vertical electric field [3,4]. This represents a striking difference with respect to single-layer graphene and makes bilayer graphene a much more suitable candidate for successful application in electronics in comparison to monolayer graphene. An insulating state induced by a vertical electric field has actually been reported in dual-gated bilayer graphene devices [5,6]. In these studies, SiO_2-supported graphene was employed and the temperature-dependence of the low-T resistivity has been addressed as evidence of the gapped state, indicating the hopping between localized states as the dominating transport mechanism. The use of ultraclean suspended bilayer graphene devices (with mobility exceeding 10^5 cm^2 V^{-1} s^{-1}) gave the possibility to observe even more subtle effects, such as interaction-induced reconstruction of the low-energy spectrum [7] and spontaneous broken-symmetry insulating states [8–10]. Nevertheless, the literature is lacking when considering *h*-BN-supported bilayer graphene, a system that can be considered halfway between SiO_2-supported and suspended graphene for what concerns the electron mobility and the possibility of having access to intrinsic phenomena. Our study aims to characterize the transport mechanisms in *h*-BN-supported bilayer graphene at zero magnetic field, for different ranges of temperature and carrier density. The determination of the temperature dependence of the resistivity (conductivity) is employed as the main tool to identify different transport regimes.

We performed four-probe electrical transport measurements on an eight-contact Hall bar made of bilayer graphene, obtained by mechanical exfoliation and deposited on top of an *h*-BN flake [see left inset in Fig. 1(a)]. A second *h*-BN flake was placed on top of graphene after Ti/Au contacts were defined by e-beam lithography and evaporated. The lower *h*-BN provides a ultraflat substrate for graphene, thanks to which the mobility can reach remarkably high values (exceeding 4×10^4 cm^2 V^{-1} s^{-1}). The uppermost layer is intended to protect the graphene flake from contamination and preserve its quality over a long time. The left inset in Fig. 1(a) shows an optical microscopy image of the sample; the uppermost *h*-BN flake is clearly visible on top of the graphene/lower-*h*-BN mesa and the metallic contacts. The bilayer nature of the graphene flake was confirmed by integer quantum Hall measurements, showing quantized plateaus in ρ_{xy} at filling factor $\nu = 4,8,12,\ldots$.

The ability to continuously tune the carrier density from the holes' to the electrons' side, through the charge neutrality point by applying a gate voltage, is unique to graphene devices on insulating substrate. Figure 1(a) shows the field effect measurements of longitudinal resistivity as a function of gate voltage at different temperatures from 300 mK to 50 K. Close to the maximum resistivity ($V_g = V_D \approx 0.5$ V), corresponding to the bands' degeneracy, the data show an insulating behavior; i.e., $d\rho/dT < 0$. At $V_g - V_D \approx \pm 5$ V, corresponding to a carrier density $n = n_c \approx \mp 2.5 \times 10^{11}$ cm^{-2} [from low-field Hall measurements; see open circles in Fig. 1(a)], the curves show a temperature-independent crossing point [see right inset in Fig. 1(a)]. Further away from the neutrality point ($|V_g - V_D| > 5$ V) a metallic behavior $d\rho/dT > 0$ is clearly observed for the curves above 10 K. We stress that such a metallic regime has not been reported in previous works on SiO_2-supported bilayer graphene such as Refs. [11,12].

The observation of a T-independent crossing point suggests the presence of a density-driven metal-to-insulator transition (MIT) of the two-dimensional electron gas, analogous to what has been observed in semiconductor-based devices [13,14]. In such systems the interplay between strong Coulomb interactions and random disorder leads to a zero-T quantum phase transition (QPT) between an insulating and a metallic state when the carrier density exceeds a critical value. The phenomenology we observe in our encapsulated bilayer is

*Corresponding author: sergio.pezzini@unipv.it

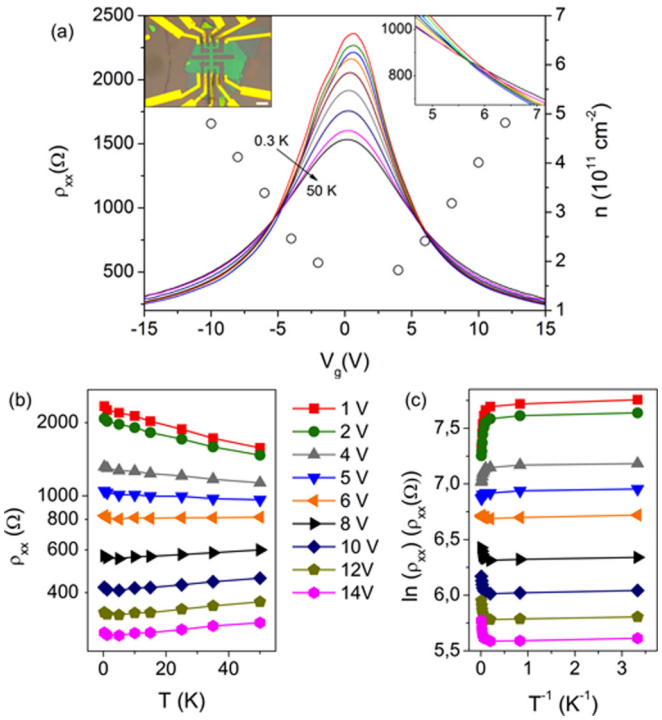

FIG. 1. (Color online) (a) Solid lines: Longitudinal resistivity as a function of gate voltage, at T from 300 mK to 50 K. Open circles: Carrier density as a function of gate voltage, from low-field Hall measurements at $T = 0.3$ K. Left inset: Optical image of the device. The aspect ratio of the sample is 6; the scale bar is 5 μm. Right inset: ρ_{xx} (Ω) vs $V_g(V)$ in the vicinity of the crossing point for e^-. (b) $\rho_{xx}(T)$ for increasing gate voltage, from top to bottom (for clarity only curves in the e^- side are reported; the same qualitative behavior is observed for h^+). (c) $\ln(\rho_{xx})$ vs T^{-1} for the same gate voltages in (b).

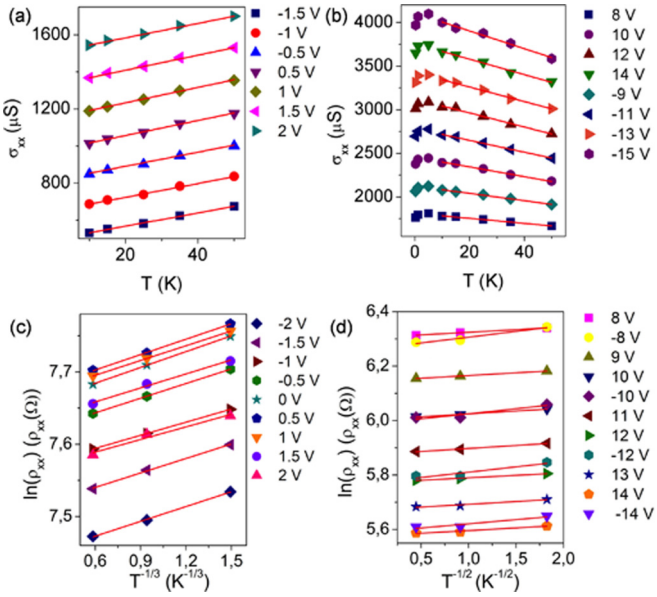

FIG. 2. (Color online) (a) Linear conductivity as a function of temperature in the vicinity of the charge neutrality point (data at different V_g are offset for clarity). (b) Conductivity as a function of temperature for $n > n_c$. Note the linearity in the ballistic region. (c) $T^{-1/3}$ dependence of $\ln(\rho_{xx})$ close to the neutrality point(±2 V range). (d) $T^{-1/2}$ dependence of $\ln(\rho_{xx})$ for $n > n_c$. The red lines are linear fits to our data.

qualitatively reminiscent of this behavior. Nevertheless, a careful analysis of the data allows us to rule out the possibility of a proper zero-T MIT for our sample. Figures 1(b) and 1(c) show respectively ρ_{xx} as a function of T and $\ln(\rho_{xx})$ as a function of $1/T$, for increasing gate voltages, driving the system through n_c on the electrons' side. In both figures the transition from $d\rho/dT < 0$ to $d\rho/dT > 0$ is clearly observable with increasing gate voltage at $T \geqslant 10$ K (while below 10 K the curves show a different dependence with n and T; we will comment thoroughly on this). The first remark we make is that our data span a resistivity range of about one order of magnitude $[2 \times 10^2\ \Omega \lesssim \rho_{xx}(n,T) \lesssim 2 \times 10^3\ \Omega]$, while in systems exhibiting MIT at low temperature the resistivity varies over a much wider range of almost 10^5 when passing from the insulating to the metallic state. Moreover the T-independent "separatrix" corresponding to the critical density for a MIT is expected to appear at $\rho_{xx}(n_c) \approx 3h/e^2$ [15], while in our sample $\rho_{xx}(n_c) \approx 900\ \Omega$, which is almost two orders of magnitude smaller. In addition, we could not find any scaling law indicating universality of the $\rho(T)$ curves in the vicinity of n_c, which is something distinctive of a MIT and this fact rules out the possibility of a proper zero-T MIT. Even though we are making use of ultraflat h-BN as a substrate, the disorder potential in our supported sample seems to be too strong for this kind of QPT to appear.

In the following we will individuate four different transport regimes, separated by density ($n = n_c$) and temperature ($T \approx 10$ K) boundaries. Each panel in Fig. 2 refers to one of them and shows how the data were fitted in order to get to the physical interpretation we will describe in the text.

In the vicinity of the charge neutrality point, the conductivity [calculated via the tensorial relation $\sigma_{xx} = \rho_{xx}/(\rho_{xx}^2 + \rho_{xy}^2)$] increases with temperature, showing a nearly perfect linear dependence between 10 K and 50 K [see Fig. 2(a)]. This is expected as a consequence of the parabolic energy-momentum relation of bilayer graphene, that results in a constant density of states. It is straightforward to calculate the minimum conductivity as $\sigma_{\min} = e\mu \int D(E)[f(E,T) - f(E,T=0)]dE = [4\ln(2)e\mu mk/\pi\hbar^2] \times T$, where $D(E)$ is the density of states, $f(E,T)$ is the Fermi-Dirac distribution function, m is the effective mass, μ is the mobility, and the factor 4 accounts for spin and valley degeneracy. Assuming $m = 0.03 \times m_e$ [16] and $\mu = \mu_{\text{Hall}}(V_g = 4\text{ V}) = 30\,000$ cm^2 V^{-1} s^{-1} (Hall mobility measured in the vicinity of the neutrality point), we obtain $\sigma_{\min} = (13.5\ \frac{\mu S}{K}) \times T$. Our data fit well to a linear σ_{xx} vs T dependence, with slope varying from 3.5 to 4 $\frac{\mu S}{K}$ for applied gate voltage in a ±2 V range around the neutrality point. The same method was used in Ref. [7] to fit the conductivity of a suspended bilayer sample, which resulted compatible with $m = 0.03 \times m_e$. Our fit indicates a suppression of the effective mass down to $m \approx 0.009 \times m_e$ at the neutrality point, in accordance with recent calculations [17] and experiments on SiO_2-supported samples [18].

For $n > n_c$ the conductivity decreases linearly with temperature up to 50 K [see Fig. 2(b)], following the behavior expected for a ballistic conductor even at remarkably high temperature. In this second regime, the dominant elastic scattering mechanism is expected to be electron scattering by Friedel oscillations caused by short-range impurities [19], giving a quantum correction to the conductivity $\delta\sigma = \sigma_0(1 + 3F_0^\sigma/1 + F_0^\sigma)T/T_F$ (where σ_0 is the Drude's conductivity and F_0^σ is the Fermi-liquid interaction parameter in the triplet channel), that determines the linear dependence with T. The first derivative $d\sigma/dT$ [obtained from linear fits to the conductivity in the metallic regime, as shown in Fig. 2(b)] increases in absolute value with increasing carrier density [see Fig. 2(b)], in accordance with experimental studies on conventional 2DEG [20]. $d\sigma/dT$ evolves differently with respect to density in the electron and hole sides, indicating e-h asymmetry in this interaction-dominated regime. From $d\sigma/dT$ we are able to estimate an interaction parameter $F_0^\sigma \approx -0.25$ in the density range considered, where the negative sign determines the metallic slope for $n > n_c$. The minus sign is in accordance with what is reported both for monolayer graphene on SiO_2 [21] and a ballistic 2DEG in the GaAs/GaAlAs heterostructure [20], while the absolute value is halfway between those of Ref. [21] ($F_0^\sigma = -0.1$) and of Ref. [20] ($-0.4 < F_0^\sigma < -0.3$).

Ballistic conduction is expected to take place when the condition $T\tau > \hbar$ (where τ is the mean elastic scattering time) is satisfied. From the onset temperature of the linearly decreasing conductivity, we can estimate $\tau \approx 0.7$ ps. This results in a mobility $\mu = \frac{e\tau}{m} \approx 41\,500$ cm^2 V^{-1} s^{-1}, in good agreement with the Hall mobility extracted from our data at high density [$\mu(10\text{ V}) = 39\,000$ cm^2 V^{-1} s^{-1}; $\mu(15\text{ V}) = 42\,000$ cm^2 V^{-1} s^{-1}].

The low-temperature data ($T \ll 10$ K) always show $d\rho/dT < 0$, both for $n < n_c$ and $n > n_c$, in striking difference with respect to the two high-temperature regimes described above. In the vicinity of the charge neutrality point, the data follow a dependence of the type $\rho \propto \exp(T/T_0)^{-1/3}$ [see Fig. 2 (c)]; this is expected for transport in 2D for noninteracting carriers via variable range hopping (VRH) mediated by localized impurity states inside a gap [22–24]. This type of behavior has been observed in bilayer graphene in the presence of an energy-gap induced by a vertical electric field that breaks the layers' symmetry in double-gated devices [5,6]. From the linear fits shown in Fig. 2(c) we obtained a characteristic temperature $T_0 \approx 0.07$ K. Such value is actually one order of magnitude smaller then the ones reported in Ref. [5], indicating a weaker temperature dependence and a larger localization length with respect to the case of top-gated bilayer graphene devices. Conclusive evidence of the presence of a layers' asymmetry-induced gap opening would be an activated T dependence of the type $\rho \propto \exp(T^{-1})$, which is something we have not detected in our data in any temperature range. The spontaneous broken-symmetry insulating state in zero magnetic field has been reported only in ultraclean suspended bilayer devices [8,9]. We argue that the presence of an energy gap in our h-BN-supported sample would be actually obscured by potential fluctuations, which in turn produce those localized states that mostly contribute to transport via VRH in the low-T regime.

Hopping between localized states constitutes the dominant contribution to the conduction unless the thermal energy is sufficient to excite carriers above the mobility edge and populate extended states, i.e., unless kT overcomes the energy scale of the potential fluctuations. As a consequence, from the onset temperature of VRH ($T \lesssim 10$ K) we can estimate a reasonable order of magnitude for the potential fluctuations in our sample $\delta\epsilon \approx 0.9$ meV (which also gives un upper limit for the amplitude of the asymmetry gap discussed above). Indeed this energy scale is directly related to the surface density fluctuations δn by the relation $\delta\epsilon \approx h^2\delta n/8\pi m$ in bilayer graphene [25]. We estimate $\delta n \approx 2.4 \times 10^{11}$ cm^{-2}. Notably, local probing of single-layer graphene on h-BN substrate with scanning tunneling microscopy gave a similar value ($\delta n \approx 2.3 \times 10^{11}$ cm^{-2} has been reported in Ref. [26]). It is remarkable that the obtained value of δn is comparable with the charge density n_c corresponding to the T-independent crossing point. This fact suggests that the onset of the metallic behavior is likely to be triggered by a full overcoming of the density fluctuations by the electrostatically-induced carriers (i.e., $n > n_c$ actually corresponds to $n > \delta n$).

Finally, for $n > n_c$ the low-T data show a dependence of the type $\rho \propto \exp(T/T_0)^{-1/2}$. A renormalization of the exponent $1/3$ to $1/2$ is expected when Coulomb interaction between localized charges is taken into account [24]. Also in this fourth regime, the transport mechanism is VRH via localized states inside a gap, which is given by vanishing single-particle density of states at the Fermi level due to interaction. As shown in Fig. 2(d), this behavior is very well verified for any gate voltage above the T-independent crossing point. The evidence of this temperature dependence hints at the importance of the e-e (h-h) interaction above n_c, where the system clearly enters the electron (hole) regime, as opposed to the neutrality point region, where e-h puddles form and the exponent $1/3$ has been previously reported in bilayer graphene [6].

In conclusion, we thoroughly characterized the temperature dependence of the electrical resistivity (conductivity) of a bilayer graphene sample enclosed between two h-BN flakes. We were able to individuate four different regimes, that are realized by tuning temperature and density over easily

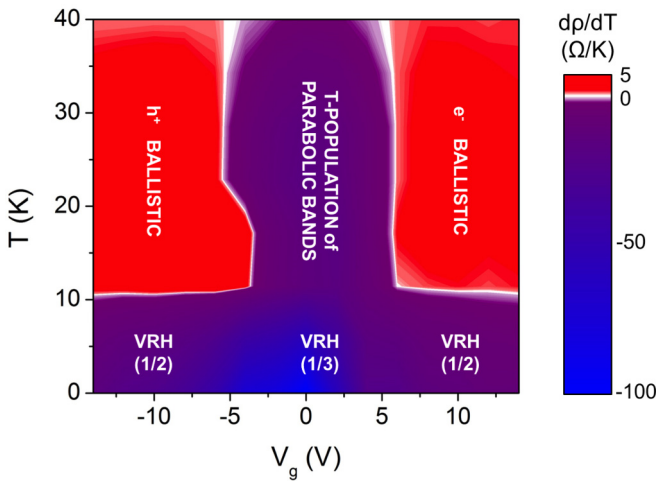

FIG. 3. (Color online) $d\rho/dT$ color map as a function of temperature and gate voltage, summarizing the main results of our study.

accessible ranges. Figure 3 summarizes our main findings. The parabolic shape of bilayer graphene's bands results in a linear insulating-like $\sigma_{xx}(T)$ in the vicinity of the maximum resistivity, which slope is compatible with a suppression of the effective mass. For $n > n_c$ ballistic transport is observed for up to 50 K; electron scattering by Friedel oscillations dominates this regime. From the first derivative of the conductivity with respect to temperature we were able to estimate a Fermi-liquid interaction constant $F_0^\sigma \approx -0.25$. The low-temperature regime is instead dominated by VRH via localized states, produced by potential fluctuations of magnitude equal to those expected for h-BN-supported graphene, with a characteristic exponent that is renormalized due to Coulomb interactions at high density. We also ruled out the possibility of a zero-T MIT and we propose an upper limit for an asymmetry-induced band gap, which seems to be obscured by potential fluctuations. We emphasize the importance of using h-BN in combination with graphene in order to have access to this variety of transport regime in a supported bilayer sample. The coexistence of these transport regimes in the system studied is a peculiar feature. We believe that our results will stimulate theoretical investigation and further experimental works on h-BN/bilayer graphene heterostructures. Future work will be devoted to density- and temperature-dependent magnetotransport measurements, aiming at exploring the possibility of a MIT at finite magnetic field.

We are grateful to Dr. Niko Tombros for providing the sample and for useful discussions. This work has been supported by the following projects: MINECO PCT-420000-2010-008, JCYL SA226U13, FPU AP2009-2619, and USAL–Apoyo a la Investigación KBBB.

[1] E. McCann and V. I. Fal'ko, Phys. Rev. Lett. **96**, 086805 (2006).
[2] K. S. Novoselov *et al.*, Nat. Phys. **2**, 177 (2006).
[3] E. McCann, Phys. Rev. B **74**, 161403 (2006).
[4] E. McCann, D. S. L. Abergel, and V. I. Fal'ko, Eur. Phys. J.: Spec. Top. **148**, 91 (2007).
[5] J. B. Oostinga, H. B. Heersche, X. L. Liu, A. F. Morpurgo, and L. M. K. Vandersypen, Nat. Mater. **7**, 151 (2008).
[6] K. Zou and J. Zhu, Phys. Rev. B **82**, 081407(R) (2010).
[7] A. S. Mayorov *et al.*, Science **333**, 860 (2011).
[8] J. Velasco, Jr. *et al.*, Nat. Nanotechnol. **7**, 156 (2012).
[9] F. Freitag, J. Trbovic, M. Weiss, and C. Schonenberger, Phys. Rev. Lett. **108**, 076602 (2012).
[10] R. T. Weitz, M. T. Allen, B. E. Feldman, J. Martin, and A. Yacoby, Science **330**, 812 (2010).
[11] S. V. Morozov, K. S. Novoselov, M. I. Katsnelson, F. Schedin, D. Elias, J. A. Jaszczak, and A. K. Geim, Phys. Rev. Lett. **100**, 016602 (2008).
[12] K. Gopinadhan, Y. J. Shin, and H. Yang., Appl. Phys. Lett. **101**, 223111 (2012).
[13] S. V. Kravchenko, W. E. Mason, G. E. Bowker, J. E. Furneaux, V. M. Pudalov, and M. D'Iorio, Phys. Rev. B **51**, 7038 (1995).
[14] S. V. Kravchenko, D. Simonian, M. P. Sarachik, W. Mason, and J. E. Furneaux, Phys. Rev. Lett. **77**, 4938 (1996).
[15] S. V. Kravchenko and M. P. Sarachik, Rep. Prog. Phys. **67**, 1 (2004).
[16] S. Adam and S. Das Sarma, Phys. Rev. B **77**, 115436 (2008).
[17] G. Borghi, M. Polini, R. Asgari, and A. H. MacDonald, Solid State Commun. **149**, 1117 (2009).
[18] K. Zou, X. Hong, and J. Zhu, Phys. Rev. B **84**, 085408 (2011).
[19] G. Zala, B. N. Narozhny, and I. L. Aleiner, Phys. Rev. B **64**, 214204 (2001).
[20] Y. Y. Proskuryakov, A. K. Savchenko, S. S. Safonov, M. Pepper, M. Y. Simmons, and D. A. Ritchie, Phys. Rev. Lett. **89**, 076406 (2002).
[21] A. A. Kozikov, A. K. Savchenko, B. N. Narozhny, and A. V. Shytov, Phys. Rev. B **82**, 075424 (2010).
[22] N. F. Mott, Philos. Mag. **19**, 835 (1969).
[23] O. Madelung, *Introduction to Solid-State Theory* (Springer, Berlin, 1978).
[24] B. I. Shklovskii and A. L. Efros, *Electronic Properties of Doped Semiconductors* (Springer, Berlin, 1984).
[25] B. E. Feldman, J. Martin, and A. Yacoby, Nat. Phys. **5**, 889 (2009).
[26] R. Decker *et al.*, Nano Lett. **11**, 2291 (2011).